# Monitoring the Drying Process Using Multi-Temporal AVHRR Data in 1990, Huaihe River Basin, China

Atsushi Higuchi[1] , Akihiko Kondoh[2], Shinkichi Kishi[3], Teruki Fukuzono[3], and Jiren Li[4]

## ABSTRACT

Recent researches have shown that the combination of spectral vegetation indices (VIs) with thermal infrared observations may provide an effective method for parameterizing surface processes at large spatial scales. In this study, we tested a hypothesis that seasonal changes in the slope of VIs and surface temperature $T_s$ derived from the satellite remote sensing are sensitive to drying processes of surface moisture status.

Huaihe River Basin, which is the study area, is characterized by steep climatological gradient from southeast to northwest. Annual precipitation in the study area decreases from southeast to northwest.

NOAA/AVHRR (Advanced Very High Resolution Radiometer) GAC (Global Area Coverage) data over the study area for the continuous 80 days after *Meiyu* (the name of rainy season from June to July, in China) of 1990 were used to derive VIs as well as $T_s$ values, while meteorological data provided by NOAA GDS (Global Daily Summery) CD-ROM was used for analysis.

After applying radiometric and geometric correction, we evaluated the slope and intercept, i. e. $T_s$ versus VIs relationships ($T_s$/VIs). Results of this study are summarized as follows

Seasonal changes in slope and intercept derived from $T_s$ and VIs relations for agricultural fields correlate well to these of antecedent precipitation index (API). Moreover, It was clear that seasonal changes in $T_s$ versus VIs relations were not only affected by seasonal changes of land surfaces moisture status, but also sensible to the effect of irrigation practice.

## INTRODUCTION

Interactions between the land surface and the atmosphere, and the resulting exchanges of energy and water have a large effect on climate. The partitioning of energy at earth's surface, between sensible and latent heat fluxes, is strongly controlled by surface moisture status.

Recent researches have indicated that the combination of spectral vegetation indices (VIs) with thermal infrared observations is an effective method for parameterizing surface processes at large spatial scales. Fig. 1 shows an example of these studies (Nemani and Running, 1989). Concept of these studies is based on Goward *et al.* (1985) suggestion. Goward *et al.* (1985) suggested the possibility of using the rate of change in surface temperature with amount of vegetation to describe surface characteristics.

In this study, we tested a hypothesis that seasonal changes in the slope of VIs and surface temperature $T_s$ derived from the satellite remote sensing are sensitive to drying process of surface moisture status.

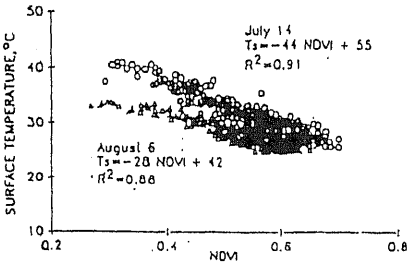


Fig. 1 Relation between surface temperature and normalized differenced vegetation index, a measure of leaf area index, from NOAA AVHRR on 6 August (Wet) and 14 July (Dry) (Nemani and Running, 1989).

[1]Doctoral Program in Geoscience, University of Tsukuba, Environmental Research Center (ERC), University of Tsukuba, 1-1-1 Tennodai, Tsukuba-shi, Ibaraki 305, JAPAN, higu@erc2.suiri.tsukuba.ac.jp

[2]Center for Environmental Remote Sensing*(CEReS)*, Chiba University, 1-33 Yayoi-cho, Inage-ku, Chiba 263, JAPAN

[3]National Research for Earth Science and Disaster Prevention, 3-1 Tennodai, Tsukuba-shi, Ibaraki 305, JAPAN

[4]Water Resources Development and Utilization Laboratory, Hohei University, CHINA

## DESCRIPTION OF THE STUDY AREA

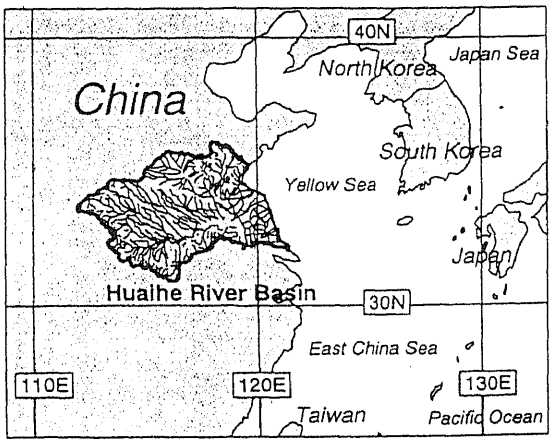


Fig. 2 Location of the Huaihe River Basin.

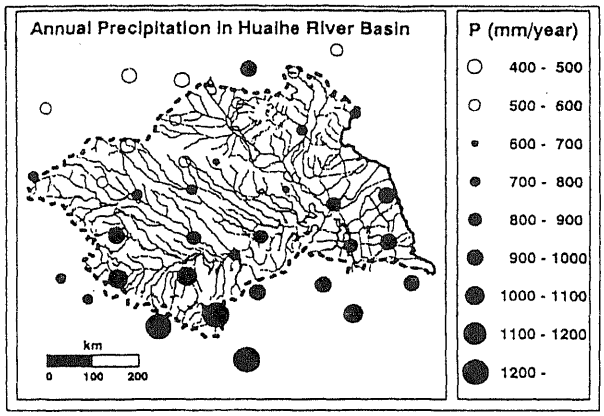


Fig. 3 Distribution of annual average precipitation in Huaihe River Basin.

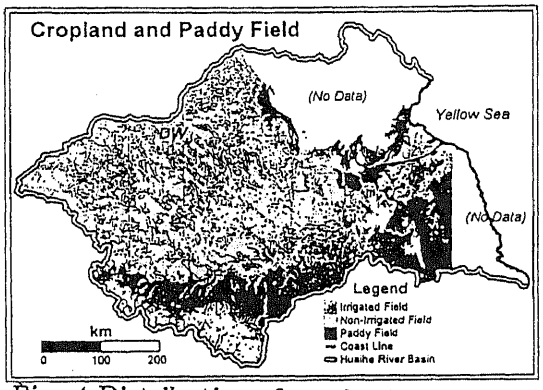


Fig. 4 Distribution of cropland and paddy field.

Huaihe River Basin (HRB) lay the south of Yellow River and the north of Yangzi River, China (Fig. 2). Catchment area of HRB is 260 $\times$ $10^3$ km$^2$, and two third of HRB is occupied by a vast stretch of a flat plain.

Climates of the study area drastically change within catchment. Southeast of HRB is in subtropical climate, and annual precipitation of this area is over 1000 mm. In contrast northwest of HRB is in semi-arid climate, and annual precipitation of this area is less than 500 mm (Fig. 3).

Vegetation and land use of the study area are generally classified into two areas (Fig. 4). Main land cover in the study area is cropland (irrigated field or non-irrigated field) in northwest, and paddy field in the southeast, although forests are present in mountainous area. Main vegetation is wheat or beans in northwest , and rice in southeast.

## METHODOLOGY

### Data source

In this study, NOAA 11 AVHRR GAC (Global Area Coverage) data over HRB for continuous 80 days (from 198 DOY (Day Of the Year) to 277 DOY) after *Meiyu* of 1990 were used.

Precipitation records were used from NOAA GDS (Global Daily Summery) CD-ROM (NOAA, 1994). Among 10000 stations, sixty stations are located within HRB.

### Radiometric correction

The raw NOAA AVHRR data are 10-bit data (from 0 to 1023 counT$_s$). In order to convert AVHRR data into radiance (channel 1 and channel 2) or brightness temperature (channel 3, channel 4, and channel 5), it is necessary to apply the radiometric correction.

Method of the radiometric correction was followed as Kidwell (1991). Moreover, we applied calibration considering the sensor degradation (Kaufman and Holben, 1993) and solar zenith angle correction for channel 1 and channel 2.

## Geometric correction

Geometric correction for registering the images on a base image employed distributed GCPs (Ground Control Points). As the base image, RESTEC (Remote Sensing Technology Center of Japan) NOAA AVHRR MOSAIC IMAGE over China which included HRB was used. We used nearest-neighbor method as interpolation method, which interpolates nearest observation point to interpolation point.

## Evaluation of Vegetation Indices (VIs), surface temperature ($T_s$), Antecedent Precipitation Index (API), and $T_s$/VIs relationships

After applying radiometric correction and geometric correction, vegetation indices (VIs) were evaluated.

$$NDVI\ (Normalized\ Difference\ Vegetation\ Index) = \frac{\rho_{ch.2} - \rho_{ch.1}}{\rho_{ch.2} + \rho_{ch.1}} \quad (1)$$

$$SAVI\ (Soil - Adjusted\ Vegetation\ Index) = \frac{\rho_{ch.2} - \rho_{ch.1}}{\rho_{ch.2} + \rho_{ch.1} + L_s}(1 + L_s) \quad (Huete,\ 1988) \quad (2)$$

$$MSAVI\ (A\ Modified\ Soil - Adjusted\ Vegetation\ Index) = \frac{\rho_{ch.2} - \rho_{ch.1}}{\rho_{ch.2} + \rho_{ch.1} + L_m}(1 + L_m) \quad (3)$$

*(Qi et al., 1994)*

$L_s$ ;soil adjustment factor ($L_s = 0.5$)
$L_m$ ;soil adjustment factor ($L_m = 1 - 2\gamma NDVI \times WDVI$)

$\gamma$ ;primary soil line parameter ($\gamma = 1.06$ )
WDVI ;Weighted Difference Vegetation Index ($WDVI = \rho_{ch.2} - \gamma\rho_{ch.1}$)

Surface temperature $T_s$ for each pixel was estimated using split-window techniques. Split-window technique was originally developed to estimate sea surface temperature (SST) by McMillin and Crosby (1984) as follows;

$$SST = 3.175 + 0.429T_3 + 2.698T_4 - 2.139T_5 \quad (McMillin\ and\ Crosby,\ 1984) \quad (4)$$

Antecedent precipitation index (API) as an index of surface moisture status by the algorithm of Choudhury *et al.*,(1987) was estimated from precipitation and temperature data within NOAA GDS, as follows;

$$API_{j+1} = K_j(API_j + P_j) \quad (5)$$

$P_j$ ;total rainfall on day $j$
$API_j$ ;the soil wetness (mm of water available for evaporation) on day $j$
$K_j$ ;soil water recession coefficient on day $j$

$$K_{j+1} = exp(-E_j/W_m) \quad (6)$$

$E_j$ ;potential evaporation (mm) on day $j$
$W_m$ ;maximum depth of soil water available for evaporation (15mm)

According to the algorithm by Nemani *et al.*,(1993), scatterplots of $T_s$ and VIs are created in 10 × 10 pixels window region (about 40 × 40 km$^2$), and the slope and intercept of upper envelope are extracted automatically.

## RESULTS AND DISCUSSION

### Response of different VIs

Fig. 5 shows a comparison between different VIs (NDVI, SAVI and MSAVI) values. According to Qi *et al.* (1994), MSAVI show the density of vegetation. When MSAVI values are close to SAVI, density of vegetation is intermediate. MSAVI values in HRB are similar to SAVI (MSAVI = 0.875123 SAVI - 0.00300534)(see Fig. 5 (c)). Vegetation over HRB indicates intermediate vegetation in the growing season. NDVI values are higher than ether SAVI or MSAVI (see Fig. 5 (a) and (b), respectively). It indicates that NDVI is affected by soil reflectance noise.

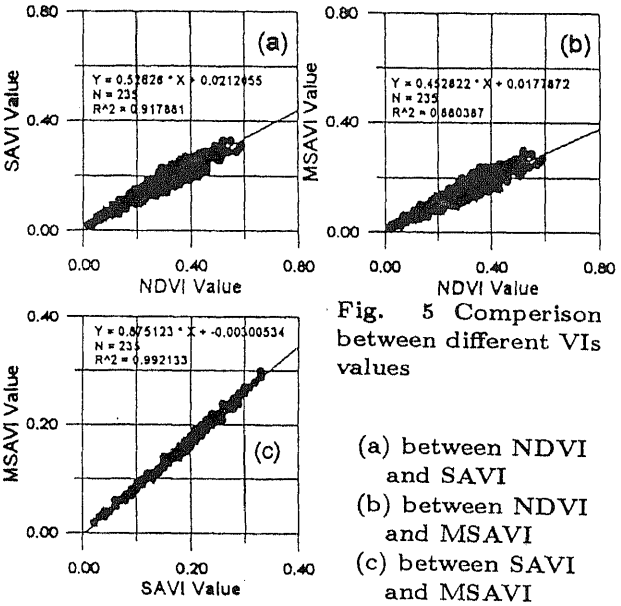


Fig. 5 Comperison between different VIs values

(a) between NDVI and SAVI
(b) between NDVI and MSAVI
(c) between SAVI and MSAVI

### Relationship between $T_s$ and VIs relations and Antecedent Precipitation Index (API) for different land uses

If the land surfaces are wetted by rainfall, much of the absorbed short radiation energy is consumed in evaporation (latent heat flux) and $T_s$ values would show no difference between soils and leaves, resulting weak or no relationships between $T_s$ and VIs. Inversely, if the land surfaces are being dry, steep relation in $T_s$/VIs because of changes in the partitioning of energy between sensible and latent heat fluxes. Are these assumptions confirmed in this study area?

Fig. 6 shows the time series of slope value and API in selected GDS stations. Climate condition in these GDS stations changes from semi-arid to subtropical, from Fig. 6 (a) to (d). During the *Meiyu* period, the slope values are relatively small in each station. In the rainless period after *Meiyu* between DOY 230 and DOY 250, the slope gradually becomes steep (large minus value). This change can be regarded as the drying process of ground surface. Because insolation is strong at the period just after the *Meiyu*, several no rainy days are enough to suppress soil evaporation. Dominated transpiration and suppressed soil evaporation make the slope in $T_s$/VI relationship steep.

Fig. 7 shows the spatial and temporal changes of the slope values in selected DOYs. Light color shows the dry condition, and the black (zero intensity) means the sea, cloudy condition, or out of image. In the rain period on DOY 212 (30 Jul.), slope distribution shows that middle of the basin is in wet condition. In the western and southern part of the basin, slope indicates the relatively dry condition. On DOY 240 (29 Aug.), there is a westward trend from wet to dry condition in the slope distribution. This slope distribution shows that the northern edge of the basin is in wet condition. It may be attributed to the irrigation practice, because rainfall do not occur this region from 10 days before. The general trend is from wet condition in eastern region to dry condition in western region, which is compatible annual precipitation distribution referred in Fig. 3. It offers the evidence that spatial and temporal slope values in $T_s$/VIs relationships can apply to the "useful indicator" monitoring drying process of surface moisture status .

## CONCLUSION

This study tested a hypothesis that seasonal changes in the slope of VIs and $T_s$ derived from the satellite remote sensing are sensible to drying process of surface moisture status. The time series of the slope values in $T_s$/VIs relationships were well corresponded to the API as an indicator of surface dryness. It indicated the usefulness of $T_s$/VIs relationships to estimate surface moisture status or to monitor drying process.

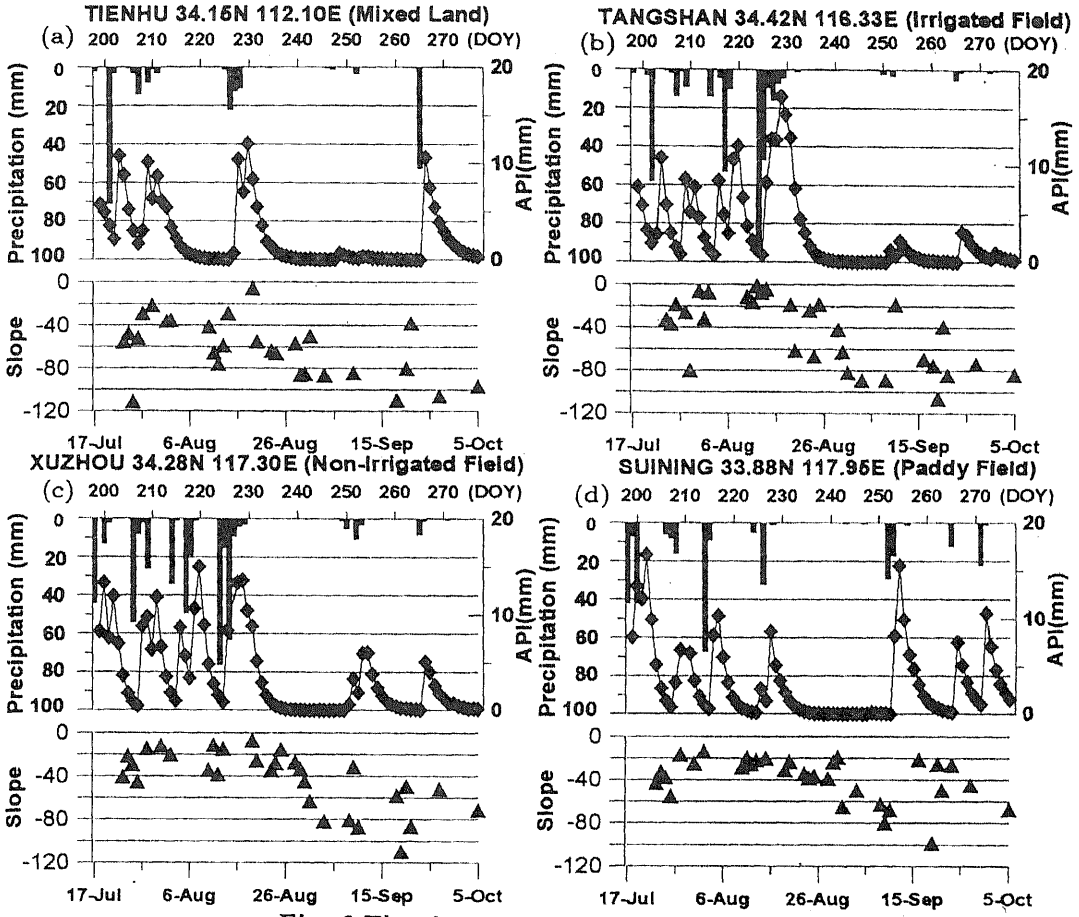


**Fig. 6 The changes in dayly precipitation, antecedent precipitation index (API) and the slope of $T_s$/VI relationship in (a) mixed land, (b) irrigated field, (c) non-irrigated field, and (d) paddy field.**

## REFERENCE


Choudhury, B. J., Owe, J., Goward, S. N., Golus, R. E., Ormsby, J. P.,Chang, A. T. C., and Wang, J. R. (1987): Quantifying spatial and temporal variabilities of microwave brightness temperature over the U. S. Southern Great Plains, *Int. J. Remote Sensing*, **8**: 177-191

Goward, S. N., Cruickshanks G. D., and Hope A. S. (1985): Observed relation between thermal emission and reflected spectral radiance of a complex vegetated landscape, *Remote Sens. Environ.*, **18**: 137-146.

Huete, A. R. (1988): A soil-adjusted vegetation index, *Remote Sens. Environ.*, **25**: 295-309.

Kaufman, Y. J. and Holben B. N. (1993): Calibration of the AVHRR visible and near-IR bands by atmospheric scattering, ocean glint and desert reflection, *Int. J. Remote Sensing*, 14: 21-52.

Kidwell, K. B. Ed. (1991): NOAA POLAR ORBITER DATA USERS GUIDE (TIROS-N, NOAA-6, NOAA-7, NOAA-8, NOAA-9, NOAA-10, NOAA-11, AND NOAA-12),NATIONAL OCEANIC AND ATMOSPHERIC ADMINISTRATION NATIONAL ENVIRONMENTAL SATELLITE, DATA, AND INFORMATION SERVICE NATIONAL CLIMATRIC DATA CENTER SATELLITE DATA SERVICE DIVISION.

McMillin, L. M. and Crosby D. S. (1984): Theory and validation of the multiple window sea surface temperature,*J. Geophys. Res.*,**89,C3**: 3655-3661.

Nemani, R. R., and Running S. (1989): Estimation of surface resistance to evapotranspiration from NDVI and thermal-IR AVHRR data,*J. Appl. Meteor.*,**28**: 276-284.

Nemani, R, R., Pierce, L., Running, S., and Goward, S. (1993): Developing satellite-derived estimates of surface moisture status, *J. Appl. Meteor.*, **32**: 548-557.

Qi, J., Chehbouni A., Huete A. R., Kerr Y. H., and Sorooshian S. (1994): A modified soil vegetation index,*Remote Sens. Environ.*,**48**:119-126.

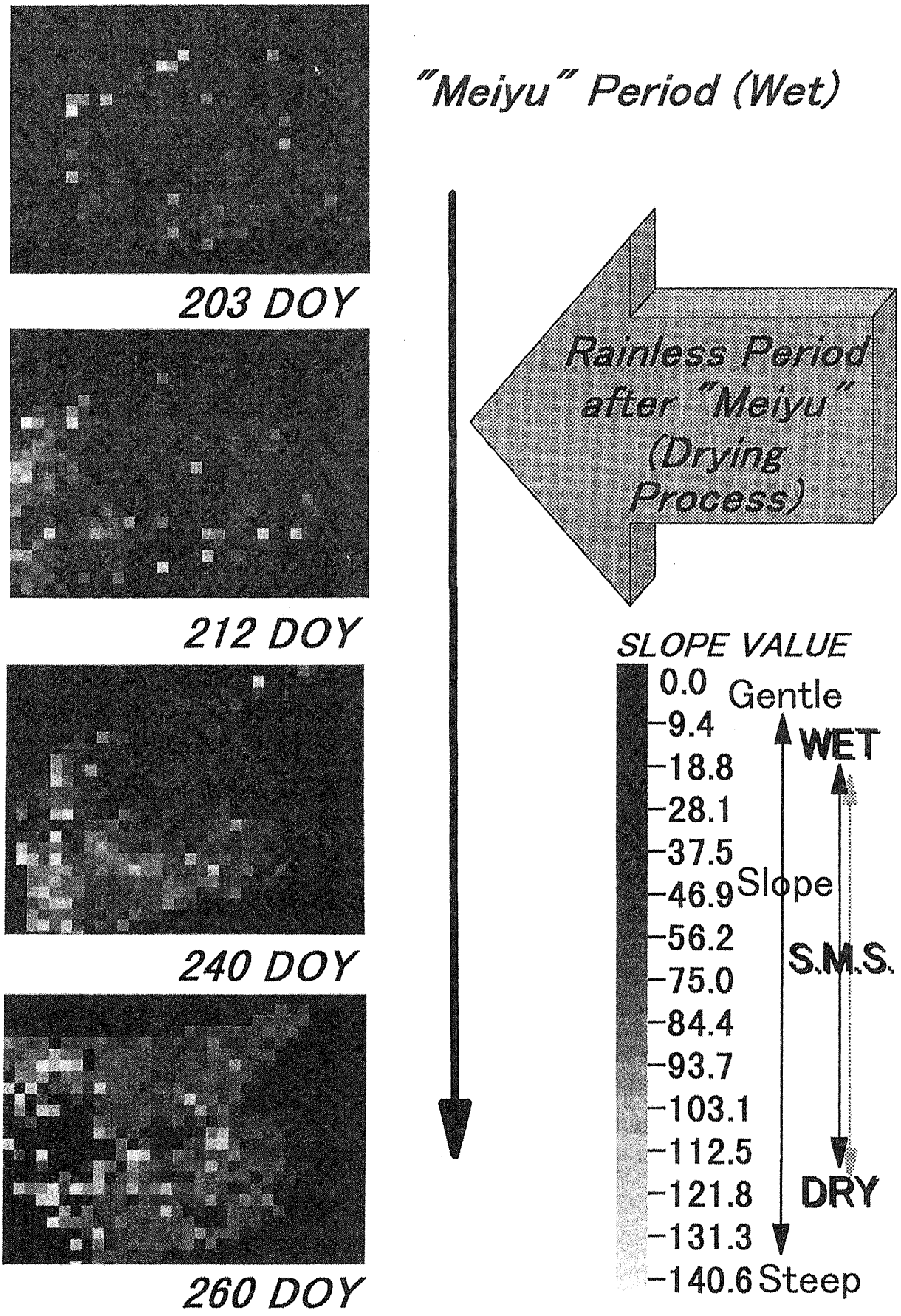


Fig. 7 Time series of spatial slope values which represent the drying process.
(S.M.S. means Surface Moisture Status.)